

HORIZON EUROPE PROGRAMME  
HORIZON-CL4-2023-DIGITAL-EMERGING-01-33

GA No. 101135196

## Developing New 2D Materials and Heterostructures for Printed Digital Devices



### 2D-PRINTABLE - Deliverable report

#### D1.5. – Production of novel 2D nanosheets by LPE, EE, CE.



Funded by  
the European Union

<b>Deliverable No.</b>	D1.5	
<b>Related WP</b>	WP 1	
<b>Deliverable Title</b>	Production of novel 2D nanosheets by LPE, EE, CE.	
<b>Deliverable Date</b>	2025-09-30	
<b>Deliverable Type</b>	REPORT	
<b>Dissemination level</b>	Public (PU)	
<b>Author(s)</b>	Joka Buha (BeD)	2025-08-25
	Shixin Liu (TCD)	2025-09-03
	Kevin Ralph Synnatschke (TUD)	2025-09-08
	Claudia Backes (UKa)	2025-09-08
<b>Checked by</b>	Francesco Bonaccorso (BeD)	
<b>Reviewed by</b>	Zdenek Sofer (VSCHT)	2025-09-10
	Xinliang Feng (TUD)	2025-09-19
	Ali Shaygan Nia (TUD)	2025-09-19
<b>Approved by</b>	Jonathan Coleman (TCD) - Project Coordinator	
<b>Status</b>	Final	
		2025-09-19

### Document History

Version	Date	Editing done by	Remarks
V1.0	2025-09-08	Authors	
V1.1			
V2.0	2025-09-10	WP1 Leader	
FINAL	2025-09-19	Reviewers	

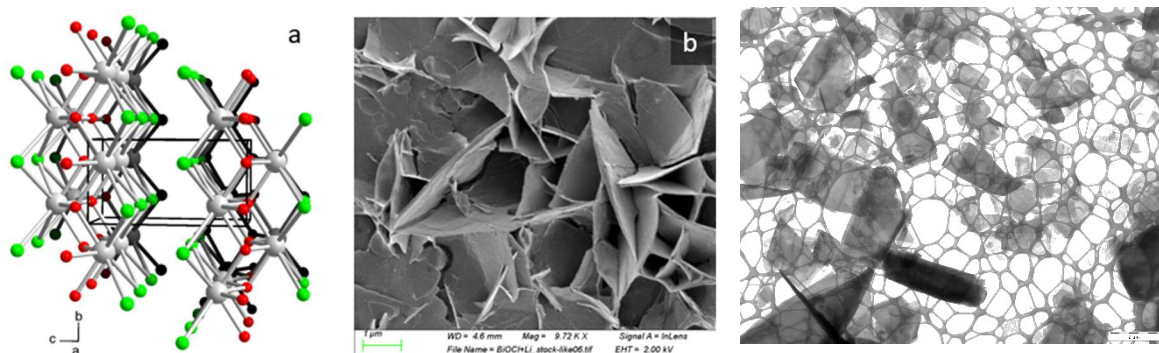
### Project Scientific Abstract

The 2D-PRINTABLE project aims to integrate sustainable large-scale liquid phase exfoliation techniques with theoretical modelling to efficiently produce a wide range of new 2D materials (2DMs), including conducting, semiconducting, and insulating nanosheets. The focus includes developing the printing and liquid phase deposition methods required to fabricate networks and multicomponent heterostructures, featuring layer-by-layer assembly of nanometer-thick 2DMs into ordered multilayers. The goal is to optimize these printed networks and heterostructures for digital systems, unlocking new properties and functionalities. The project also seeks to demonstrate various printed digital devices, including proof-of-principle, first-time demonstration of all-printed, all-nanosheet, heterostack light-emitting diodes (LEDs). In conclusion, 2D-PRINTABLE will prove 2D materials to be an

indispensable material class in the field of printed electronics, capable of producing far-beyond-state-of-the-art devices that can act as a platform for the next generation of printed digital applications.

## Public summary

This deliverable reports on advances made with different methodologies of exfoliation and on novel 2D materials exfoliated from the stock of layered crystals synthesized within WP1. Among many 2D materials identified and synthesized in first months of this project, we have then focused on materials deemed most technologically relevant, considering also the abundance and availability of the source elements. Liquid phase exfoliation using ultrasonication has been utilized to obtain high-quality nanosheets of several transition metal oxyhalides, binary and ternary chalcogenides and other layered and nonlayered materials. In some cases, functionalization aimed at improving the colloidal stability of NSs and exfoliation of bulk material have been combined into a single step. The use of high shear mixer has also been used with mixed success in order to produce larger quantities of NSs in a relatively short processing time. Significant advancement has been made in both chemical and electrochemical exfoliation of several different materials in which high quality NSs of very high aspect ratio have been produced.



*Model of the crystal structure of bismuth oxychloride (BiOCl) on the left and a scanning electron microscopy image of BiOCl nanosheets produced by chemical exfoliation (middle). High aspect ratio iron oxychloride nanosheets produced by ultrasonication (transmission electron image on the right)*

## Contents

1	Introduction.....	7
2	Methods .....	8
2.1	Background .....	8
2.2	Procedures .....	8
2.3	Data Analysis.....	10
3	Results & Discussion.....	11
3.1	LPE of layered and non layered materials .....	11
3.1.1	LPE of transition metal oxyhalides .....	11
3.1.2	LPE of $\text{AsSbS}_3$ , $\text{As}_2\text{S}_3$ , $\text{SnGe}$ , $\text{As}_4\text{S}_4$ , and $\text{K}_3\text{Fe}(\text{CN})_6$ .....	13
3.1.3	LPE or $\text{TaS}_2$ and GeMe .....	14
3.2	Electrochemical and chemical exfoliation of novel 2D materials.....	16
3.3	Contribution to project (linked) Objectives .....	20
3.4	Contribution to major project exploitable result.....	20
4	Conclusion and Recommendation .....	21
5	References.....	22
6	Acknowledgement.....	23
7	Appendix A - Quality Assurance Review Form .....	24

## List of Figures

**Figure 1.** The principle of material disintegration/ homogenization in Silverson homogenizer. Source and copyright: [www.silverson.com/](http://www.silverson.com/)

**Figure 2.** a) TEM image of VOCl NSs exfoliated by sonication assisted LPE in toluene with oleylamine as surfactant. b) Electron diffraction pattern from one of the VOCl NSs in the [001] zone axis. c) XRD patterns from bulk crystal and exfoliated material compared, both indexed according to VOCl crystal structure PANICSD:98-002-7011. d) TEM image of VOCl NSs exfoliated by sonication assisted LPE in chloroform. e) model of VOCl crystal structure. f) Raman spectra of bulk and exfoliated VOCl.

**Figure 3.** a) TEM image of TiOCl NSs exfoliated using a high shear mixer. b) selected area electron diffraction pattern from one of the NSs oriented in [001] direction and indexed according to orthorhombic crystal structure PANICSD:98-003-9314. c) model of TiOCl crystal structure where a gap between Cl layers, where cleavage is expected to occur, can be appreciated. d) AFM statistical analysis of over 100 TiOCl flakes showing that most are just over 8 nm thick. e) XRD pattern from the exfoliated TiOCl also indexed according to orthorhombic crystal structure. f) Raman spectra from bulk and exfoliated TiOCl.

**Figure 4.** a) TEM image of FeOCl NSs exfoliated in toluene in the presence of oleylamine as surfactant. b) Selected area electron diffraction pattern from one of the NSs indicating the [001] orientation observed also with all NSs examined in this way, confirming that the exfoliation of bulk crystal takes place perpendicular to c axis of the FeOCl orthorhombic crystal structure (panel c). d) Electron diffraction pattern from an assemble of NSs indexed according to orthorhombic FeOCl structure PDF 01-072-0619. e) Raman spectra of bulk and exfoliated NSs. f) TEM image of FeOCl NSs exfoliated initially in chloroform without the presence of surfactant.

**Figure 5.** Novel 2D materials produced by sonication-assisted liquid-phase exfoliation (A) Ink dispersion of 2D As<sub>4</sub>S<sub>4</sub>, TEM images of (B) AsSbS<sub>3</sub>, (C) As<sub>2</sub>S<sub>3</sub>, and (D) SnGe, respectively.

**Figure 6.** LPE TaS<sub>2</sub> in NMP. A-C) Fitted XPS Ta4f core level spectra of (A,B) different starting materials and (C) powder 1 after inert tip exfoliation and centrifugation in NMP. D-E) Electron diffraction of (E) the starting material powder 1 and (B) powder 1 after inert tip exfoliation and centrifugation in NMP. The insets show the cumulative counts as function of radius. F) Extinction spectra of size-selected NS dispersions derived from the 2 different powders showing a distinct profile which can be related to the polytype. G) Example degradation kinetics of intermediate-sized fractions produced from different powders and/or conditions after exposure of the samples to ambience. H) Rate constants of the degradation plotted as function of centrifugation conditions which are represent different NS sizes/thicknesses.

**Figure 7:** LPE of GeMe in NMP. A) Scheme of the synthesis of GeMe. B) Raman-PL spectra of the bulk material with 532 nm excitation. C) AFM of GeMe NSs after inert exfoliation in NMP using bath sonication and purification by centrifugation. D) Normalised extinction spectra of a dispersion and a NS network. E) Normalised PL spectra of the samples in (D) after excitation with 532 nm.

**Figure 8.** SEM images of novel materials, including MoWSe<sub>2</sub>, InSe, and HfSe<sub>3</sub>.

**Figure 9.** Photoluminescence measurement results of electrochemically exfoliated NSs.

**Figure 10.** The schematic illustration of basic principles of chemical exfoliation.

**Figure 11.** a) model of crystal structure of BiOCl. b) SEM image of BiOCl NSs exfoliated by ultrasonication following intercalation with NaH in water.

**Figure 12.** SEM images of BiOCl NSs obtained by different procedures involving either a) ultrasonication alone or ultrasonication following intercalation of bulk crystals by Li, Na or LiH in different solvents, as indicated on each panel.

**Figure 13.** UV-Vis absorption spectra of chemically exfoliated BiOCl NSs. (a) Comparison of the sediment fraction (after centrifugation) and the corresponding supernatant. (b) BiOCl treated with NaH in IPA, showing an additional feature at  $\sim$ 270 nm but no change in the optical band gap. (c, d) Spectra of BiOCl treated with Na and NaH in different solvents, exhibiting significant changes indicative for partial decomposition, phase transformation, or reduction of the starting material.

## 1 Introduction

Liquid phase exfoliation (LPE) of layered 2D materials to produce inks is a cost-effective and sustainable method of obtaining large volumes of ready-to-print inks and the focus of nearly all partners withing WP1. The computational screening identified easily exfoliable materials and more than 100 of those had been synthesized in the bulk form. By using and developing different methods we have so far exfoliated more than 20 novel 2D materials never accessed before in low dimensional form. Following the preliminary results reported in earlier deliverables and milestones, emphasis was placed on technologically most relevant materials. Firstly, we evaluated the quality of the obtained nanosheets (NSs) (e.g. defect-free high aspect ratio NSs are desired for semiconductor and also other components of all-printed device). Secondly, we work on the scalability, i.e., ensuring that those materials and their unique properties can be taken outside of lab and produced also on a larger scale and meet future market demands. This deliverable reports on progress made on those objectives, highlight challenges encountered and proposes future activities to successfully reach the objectives of the project.

## 2 Methods

### 2.1 Background

The exfoliation of different 2D materials was performed following several different methods and protocols. At BeD, TCD and Uka sonication assisted LPE has been optimized to produce NSs of several novel 2D materials. Additionally at BeD, new methodology of LPE has been explored to simplify and reduce the time needed to produce appreciable quantity of NSs. At TCD, TUD and UKa, methods of chemical (CE) and electrochemical (EE) exfoliation have been optimized and applied also to new materials and yielding NSs of high aspect ratio.

### 2.2 Procedures

At BeD transition metal oxyhalides such as vanadium oxychloride (VOCl), titanium oxychloride (TiOCl) and iron oxychloride (FeOCl) were exfoliated from their respective bulk materials using the established sonication-assisted LPE procedure, performed in different solvents and in the presence of surfactants added to the solvent. The sonication was performed for 8 hours and the exfoliated material was separated from the unexfoliated one and larger flakes by means of centrifugation. This procedure usually affords a small amount of exfoliated material sufficient for characterization, optimization of the exfoliation process and some limited film deposition/device fabrication trials. The feasibility of industrial scale production of 2D materials using a proprietary wet-jet milling (WJM) technology has been demonstrated by BeD and reported previously (M4).

In order to diversify the exfoliation methods and bridge the gap in obtainable quantities between sonication assisted LPE and WJM, we attempted exfoliation also by using a high shear mixer of type Silverson, which can be used to process larger quantities of material in a very short time. Unlike conventional mixers with propeller-like blades, the high shear mixer we used is equipped with particular types of high shear work heads that allow for quick disintegration and homogenization of material. The material in solvent is lifted off the bottom of mixing vessel by turbulent flow of the liquid and repeatedly pushed at high pressure through a perforated screen ring (Figure 1).

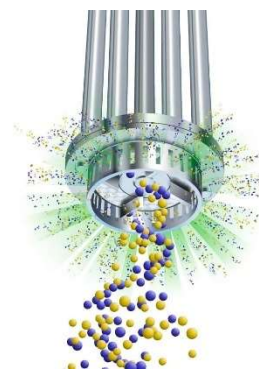


**Figure 1.** The principle of material disintegration/ homogenization in Silverson homogenizer. Source and copyright: [www.silverson.com/](http://www.silverson.com/)

The exfoliation was performed for 3 hours at mixing speed of 6500 rpm, after which the product was centrifuged to separate the exfoliated from unexfoliated material. Preliminary trials with exfoliating

graphene using Silverson mixer have shown that the exfoliation yield was inferior to that achieved by WJM. However, after centrifugation the quality of the exfoliated material is comparable to that produced by WJM or sonication. The advantage relies on the simplicity of use and relatively short processing time. The drawback, apart from the low yield, is the damage induced to some materials depending on processing parameters. As it will be reported here, prolonged homogenization using Silverson mixer causes amorphization of an already exfoliated material in some cases, while in other cases such as  $\text{Mo}_{0.5}\text{W}_{0.5}\text{Se}_2$  alloy (data not included in this report) fragmentation of an exfoliated material occurs creating two populations of thin NSs: exfoliated NSs with large lateral size and smaller fragments of NSs with similar thickness. These examples indicate the need to carefully optimize this method of exfoliation and highlights known challenges associated with LPE. This is one of the reasons why the partners within WP1 are developing novel protocols and pushing the limits of what can be achieved by chemical and electrochemical exfoliation.

Liquid phase exfoliation of materials such as teraarsenic tetrasulfide ( $\text{As}_4\text{S}_4$ ), potassium ferricyanide  $\text{K}_3\text{Fe}(\text{CN})_6$ , arsenic trisulfide ( $\text{As}_3\text{S}_3$ ), arsenic antimony trisulfide ( $\text{AsSbS}_3$ ) and tin germanide ( $\text{SnGe}$ ) at TCD was performed by ultra-sonication of powders in liquids under  $\text{N}_2$  atmosphere to avoid oxidation of the exfoliated NSs. Electrochemical exfoliation of molybdenum disulfide ( $\text{MoS}_2$ ), tungsten disulfide ( $\text{WS}_2$ ), tungsten diselenide ( $\text{WSe}_2$ ), indium selenide ( $\text{InSe}$ ), molybdenum tungsten diselenide ( $\text{MoWSe}_2$ ) and hafnium triselenide ( $\text{HfSe}_3$ ) was performed in ambient condition. The materials and electrolyte are described in the Results section.

The exfoliation of tantalum disulfide ( $\text{TaS}_2$ ) at Uka was performed in dried and degassed N-methyl-2-pyrrolidone (NMP) through bath sonication under argon atmosphere or tip sonication in a nitrogen filled glovebox for 7h. Unexfoliated material was first removed through centrifugation at 100 g for 2h. The supernatant was subjected to cascade centrifugation at sequentially increasing centrifugation speeds and the sediment containing size-selected fractions was collected after each step in fresh NMP. All decanting was performed inside the glovebox. Degradation kinetics were investigated after exposure to ambient conditions through extinction spectroscopy. Inert exfoliation of methyl germanene ( $\text{GeMe}$ ) was performed by bath sonication in dried and degassed NMP. An intermediate size (supernatant after centrifugation at 400 g and sediment after centrifugation at 1000 g) was subjected to morphological and structural analysis.

Chemical exfoliation of bismuth oxychloride ( $\text{BiOCl}$ ) at TUD was performed by intercalating bulk material with different cations in combination with different solvents, followed by brief ultrasonication aimed at delaminating the intercalated material. More detailed description and data from different trials are provided in results section.

The characterisation of the exfoliated 2D materials was performed using a range of standard techniques such as optical extinction spectroscopy, UV-Vis spectroscopy, scanning electron microscopy (SEM), transmission electron microscopy (TEM), X-ray diffraction (XRD), Raman spectroscopy, and atomic force microscopy (AFM).

## 2.3 Data Analysis

The spectra collected by different instruments (XRD, Raman Spectroscopy, UV-Vis Spectroscopy) were analysed using OriginPro. Microscopy images (SEM and TEM) were analysed using Fiji and Digital Micrograph software packages. Atomic force microscopy images and statistical analysis was performed by using Gwyddion software.

### 3 Results & Discussion

#### 3.1 LPE of layered and non layered materials

##### 3.1.1 LPE of transition metal oxyhalides

Oxyhalides of transition metals, such as VOCl, TiOCl and FeOCl, crystallize with orthorhombic crystal structure with distinct gap between adjacent halide layers held together by van der Waals interactions. The computational screening conducted within this WP predicts these materials to be easily exfoliable. Figure 2 presents data from sonication-assisted LPE of VOCl performed in toluene with oleylamine as surfactant (figure d shows the same material previously exfoliated in chloroform). This material has already attracted attention as cathode material for Li, Na, Mg and Al batteries due to its appreciably high theoretical capacity and structural and chemical stability. The sonication-assisted LPE produces NSs of high aspect ratio, which retain their structure as confirmed by electron diffraction (b), XRD (c) and Raman spectroscopy (f). The cleavage of the bulk crystals takes place on {001} planes coinciding with the gap between the halide layers. Attempted exfoliation of this material using a high shear mixer produced also amorphized material along with thin NSs, most likely due to the high shear forces and/or the prolonged exposure of already exfoliated NSs to those resulting also in structural damage of the material.

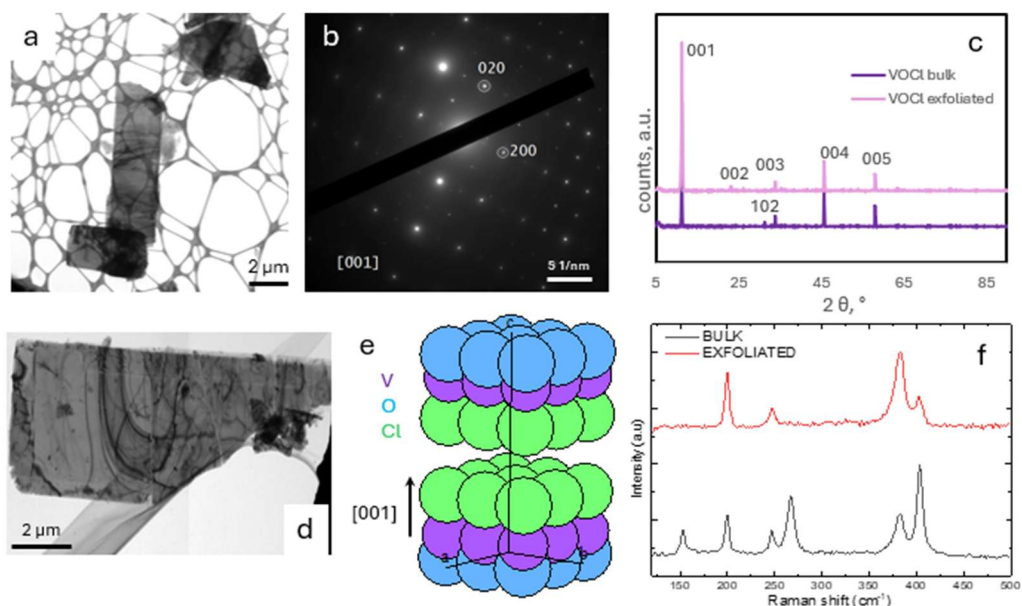


**Figure 2.** a) TEM image of VOCl NSs exfoliated by sonication assisted LPE in toluene with oleylamine as surfactant. b) Electron diffraction pattern from one of the VOCl NSs in the [001] zone axis. c) XRD patterns from bulk crystal and exfoliated material compared, both indexed according to VOCl crystal structure PANICSD:98-002-7011. d) TEM image of VOCl NSs exfoliated by sonication assisted LPE in chloroform. e) model of VOCl crystal structure. f) Raman spectra of bulk and exfoliated VOCl.

TiOCl is isostructural with VOCl and most recently also considered as anode material for multivalent ion batteries. Figure 3 summarizes the results of TiOCl exfoliation using a high shear mixer. In this case high aspect ratio NSs have been obtained without the notable degradation of the exfoliated material. The NSs obtained are similar to those obtained by sonication assisted LPE yet produced after a considerably shorter processing time.

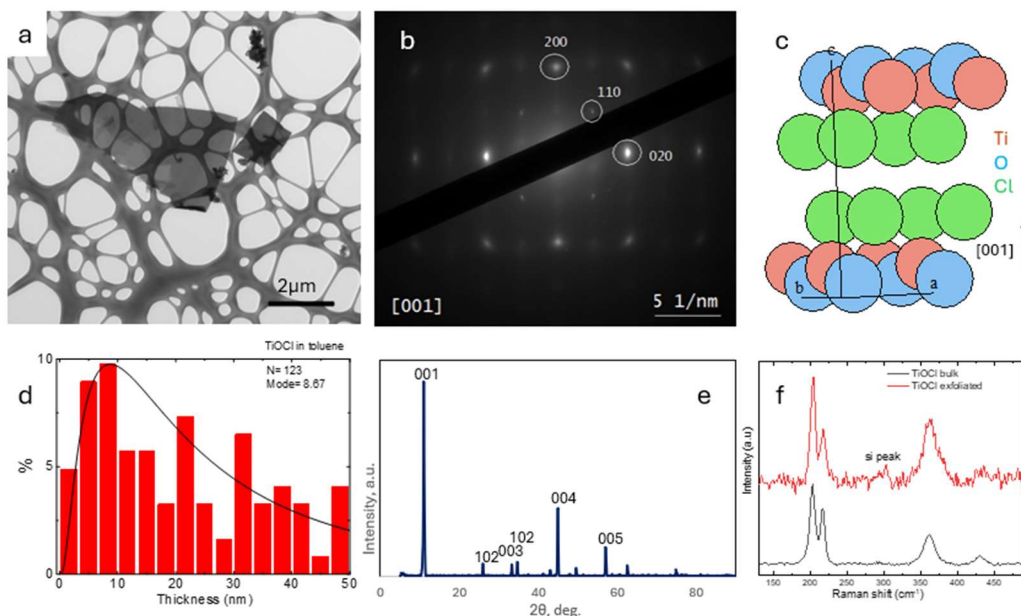


**Figure 3.** a) TEM image of TiOCl NSs exfoliated using a high shear mixer. b) selected area electron diffraction pattern from one of the NSs oriented in [001] direction and indexed according to orthorhombic crystal structure PANICSD:98-003-9314. c) model of TiOCl crystal structure where a gap between Cl layers, where cleavage is expected to occur, can be appreciated. d) AFM statistical analysis of over 100 TiOCl flakes showing that most are just over 8 nm thick. e) XRD pattern from the exfoliated TiOCl also indexed according to orthorhombic crystal structure. f) Raman spectra from bulk and exfoliated TiOCl.

FeOCl is an antiferromagnetic layered transition metal oxyhalide known for its catalytic performance and in few layers form considered for nanospintronic applications. The bulk material was exfoliated in toluene with oleylamine added as surfactant during the exfoliation, following the protocol adopted for sonication-assisted LPE. The distinctive features of the exfoliated FeOCl as compared to VOCl and TiOCl is the apparent ease of exfoliation and colloidal stability of the exfoliated material in the combination of solvent-surfactant selected for the exfoliation. As compared to same material exfoliated in chloroform alone, the NSs obtained presently in solvent of lesser polarity and surfactant added during exfoliation are more uniform in thickness and almost free from aggregation. Thin NSs of very high aspect ratio with orientation parallel to {001} planes were obtained also in this case.

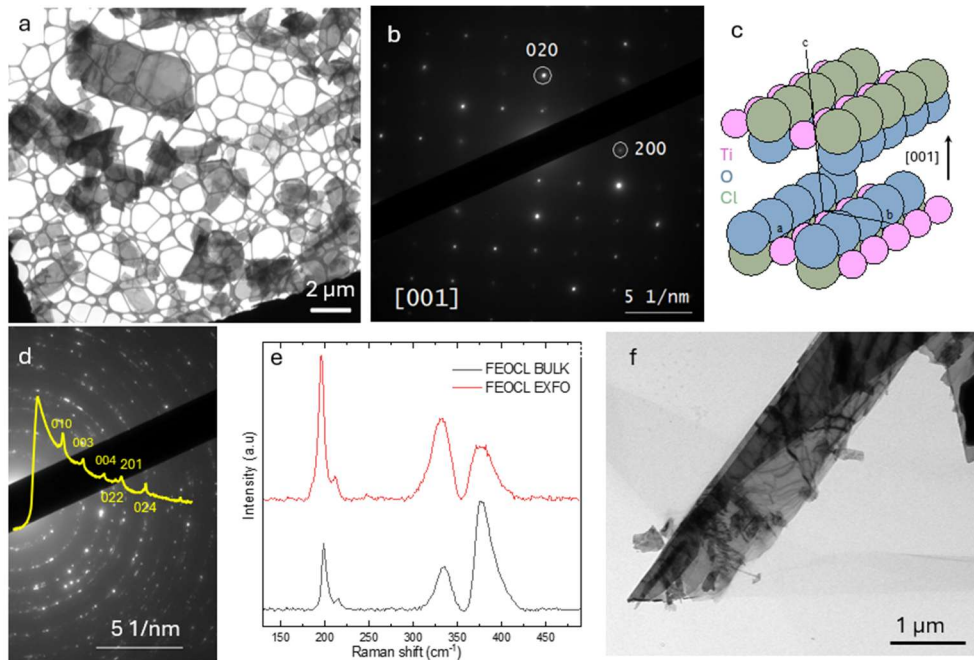


**Figure 4.** a) TEM image of FeOCl NSs exfoliated in toluene in the presence of oleylamine as surfactant. b) Selected area electron diffraction pattern from one of the NSs indicating the [001] orientation observed also with all NSs examined in this way, confirming that the exfoliation of bulk crystal takes place perpendicular to c axis of the FeOCl orthorhombic crystal structure (panel c). d) Electron diffraction pattern from an assemble of NSs indexed according to orthorhombic FeOCl structure PDF 01-072-0619. e) Raman spectra of bulk and exfoliated NSs. f) TEM image of FeOCl NSs exfoliated initially in chloroform without the presence of surfactant.

### 3.1.2 LPE of AsSbS<sub>3</sub>, As<sub>2</sub>S<sub>3</sub>, SnGe, As<sub>4</sub>S<sub>4</sub>, and K<sub>3</sub>Fe(CN)<sub>6</sub>

TCD has successfully demonstrated exfoliation of both layered and non-layered crystals such as AsSbS<sub>3</sub>, As<sub>2</sub>S<sub>3</sub>, SnGe, As<sub>4</sub>S<sub>4</sub>, and K<sub>3</sub>Fe(CN)<sub>6</sub> into 2D NSs. The dispersions of NSs are shown in Figure 5 A. The morphology of NSs is characterised by TEM, and some of them are shown in Figure 5 B-D. These materials are particularly well-suited for battery applications thanks to their theoretical high specific capacity. These materials further expand the library of available 2D materials and suggest that certain non-layered materials are suitable for exfoliation.

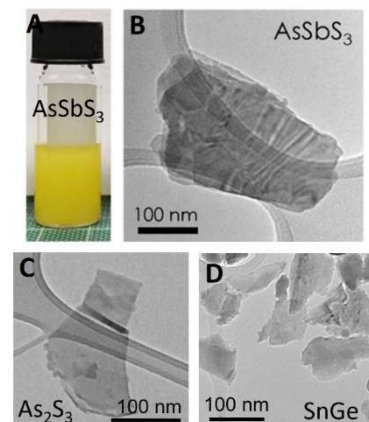


**Figure 5.** Novel 2D materials produced by sonication-assisted liquid-phase exfoliation (A) Ink dispersion of 2D As<sub>4</sub>S<sub>4</sub>, TEM images of (B) AsSbS<sub>3</sub>, (C) As<sub>2</sub>S<sub>3</sub>, and (D) SnGe, respectively.

### 3.1.3 LPE or TaS<sub>2</sub> and GeMe

Following the results reported by UKa in Deliverable 4.2, LPE of TaS<sub>2</sub> under inert conditions was further investigated. To recap previous work, we exfoliated different batches of TaS<sub>2</sub> of different (but unknown) polytype mixtures through bath and tip sonication in NMP, performed size selection and characterised the samples with extinction spectroscopy (among other techniques) after exposure to ambient condition to investigate the degradation. Further, it was found that a complete conversion to a transparent species is observed after annealing (280°C for 2h) that still has shown characteristic platelets in the SEM. Through X-ray photoelectron spectroscopy (XPS), we now found that a conversion to Ta<sub>2</sub>O<sub>5</sub> took place, which could be a promising dielectric. To understand these observations in more detail, the focus of the past 6 months was dedicated to quantifying the polytypes prior to exfoliation and their respective degradation behaviour.

The powders used for the exfoliation were characterised through XPS and electron diffraction (in a SEM). The fitted Ta4f core level spectra of two of the batches are shown in Figure 6 A,B. Both spectra show a relatively high oxide content of the samples of 43% and 76%, respectively. This demonstrates that significant surface oxidation has taken place, presumably already during shipping between the partners. The oxide content in the powder 1 after exfoliation with tip sonication and subsequent cascade centrifugation is lower (27%, Figure 6C) suggesting that the procedure resulted in some purification and actual removal of surface oxides rather than the creation of new oxidation events. Further, XPS suggests that powder 1 contains ~ 60% 1T polytype and 40% of the 2H polytype, while powder 2 consists of only 2H-TaS<sub>2</sub>. Tip sonication does not significantly change the polytype ratio for powder 1. However, we note that these results are still preliminary, and the fitting will be refined. Electron diffraction of powder 1 shows a diffraction pattern that cannot be unambiguously assigned to any pure polytype, but that agrees with literature data on a mixture of 1T/2H thus qualitatively confirming the XPS results.<sup>1</sup> After exfoliation of using tip sonication, the clear diffraction pattern is smeared out to diffraction rings located at the same radius (see inset) suggesting that disorder, e.g. due to random restacking occurred, but that the polytype mixture is widely retained.

With knowledge of the polytypes, it is worth to revisit the extinction spectra again (Figure 6F). These show some size/thickness dependence (darker and lighter traces), but more clearly, distinct spectra for the two powders of different polytype. We can thus assign that the 2H polytype shows a broad peak at 550-700 nm, while the 1T polytype has a characteristic feature at 360-390 nm and a plateau extending into the NIR region. This information is useful as it allows to qualitatively assess the polytype of unknown samples. For the different sample, degradation after exposure to ambient condition was followed through extinction spectroscopy. The kinetics of one sized fraction are shown in Figure 6G. From fitting the kinetics, we estimated the rate constants of the degradation for a range of samples, which are plotted as function of the centrifugation speed in Figure 6H. Degradation is significantly slower in the bath-sonicated samples. For the tip sonicated samples, degradation rates are similar for both powder batches, with purely 2H batch 2 being slightly less stable. For intermediate NS sizes, these degradation rates correspond to half-lives of 370 h (2H/1T) and 250 h (2H). This is comparable to degradation of LPE NiPS<sub>3</sub><sup>2</sup> and GeS,<sup>3</sup> and slower than for black phosphorus<sup>4</sup> or TiS<sub>2</sub><sup>5</sup> prepared under similar conditions. Since 2H-TaS<sub>2</sub> is more easily accessible in the bulk form and converts more easily to

$\text{Ta}_2\text{O}_5$ , future work will be directed to making NS networks from 2H-TaS<sub>2</sub> followed by conversion to the layered oxide.

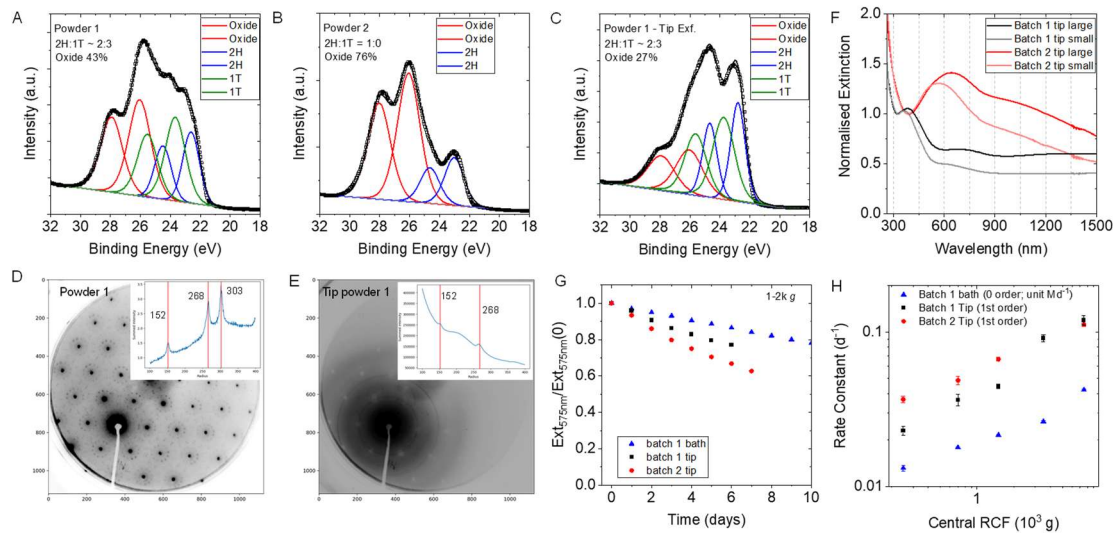


**Figure 6.** LPE TaS<sub>2</sub> in NMP. A-C) Fitted XPS Ta4f core level spectra of (A,B) different starting materials and (C) powder 1 after inert tip exfoliation and centrifugation in NMP. D-E) Electron diffraction of (E) the starting material powder 1 and (B) powder 1 after inert tip exfoliation and centrifugation in NMP. The insets show the cumulative counts as function of radius. F) Extinction spectra of size-selected NS dispersions derived from the 2 different powders showing a distinct profile which can be related to the polytype. G) Example degradation kinetics of intermediate-sized fractions produced from different powders and/or conditions after exposure of the samples to ambience. H) Rate constants of the degradation plotted as function of centrifugation conditions which are represent different NS sizes/thicknesses.

Significant progress has also been made on optimizing device stacks for light-emitting diodes (LEDs), currently focusing on electrochemically exfoliated MoS<sub>2</sub>. This demands for new materials with direct bandgap in the bulk or few-layer form. To address this, we performed inert exfoliation of GeMe in NMP. The bulk material was synthesized from CaGe<sub>2</sub> by reaction with CH<sub>3</sub>I (Figure 7A). The Raman spectra show intense photoluminescence (PL) in the bulk material observed at  $\sim 5000 \text{ cm}^{-1}$  after excitation with a 532 nm laser (Figure 7B). Centrifugation was used to narrow size and thickness distributions resulting in NS dispersions typical for LPE, as illustrated by the AFM images in Figure 7C. Typical NS lateral dimensions are in the range of  $\sim 450 \text{ nm}$ , but NSs are relatively thick ( $\sim 30 \text{ nm}$ ). Degradation in ambient condition is observed, e.g. in the NS displayed in the AFM image in Figure 7C, bottom. Extinction spectra of the NSs in dispersion, as well as NS networks after deposition display a broad maximum below 450 nm (Figure 7D). Both dispersion and film show appreciable PL centred at  $\sim 675 \text{ nm}$ , with no shift or broadening occurring on deposition (Figure 7E). Despite the discerned

degradation, this is a promising result so that future work will be dedicated to using GeMe NSs as emitters in LEDs.

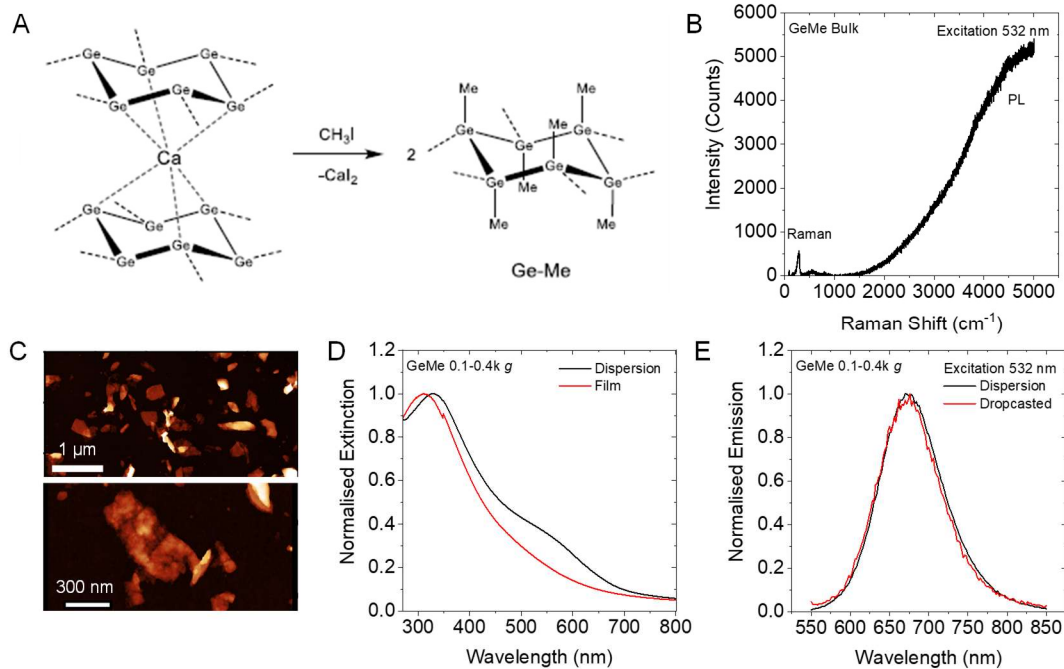


**Figure 7:** LPE of GeMe in NMP. A) Scheme of the synthesis of GeMe. B) Raman-PL spectra of the bulk material with 532 nm excitation. C) AFM of GeMe NSs after inert exfoliation in NMP using bath sonication and purification by centrifugation. D) Normalised extinction spectra of a dispersion and a NS network. E) Normalised PL spectra of the samples in (D) after excitation with 532 nm.

### 3.2 Electrochemical and chemical exfoliation of novel 2D materials

TCD performed electrochemical exfoliation on some synthetic crystals obtained from Prof. Zdenek Sofer, including  $\text{MoS}_2$ ,  $\text{WS}_2$ ,  $\text{WSe}_2$ ,  $\text{InSe}$ ,  $\text{MoWSe}_2$ , and  $\text{HfSe}_3$ . The electrolyte solution was tetrapropylammonium bromide (TPAB) and propylene carbonate (PC). The successful intercalation and NS size selection can be observed in SEM images as shown in Figure 8. Their morphological information was obtained by AFM, and their aspect ratios were in the range of  $10^2$  to  $10^3$ , confirming their atomic thin structures.

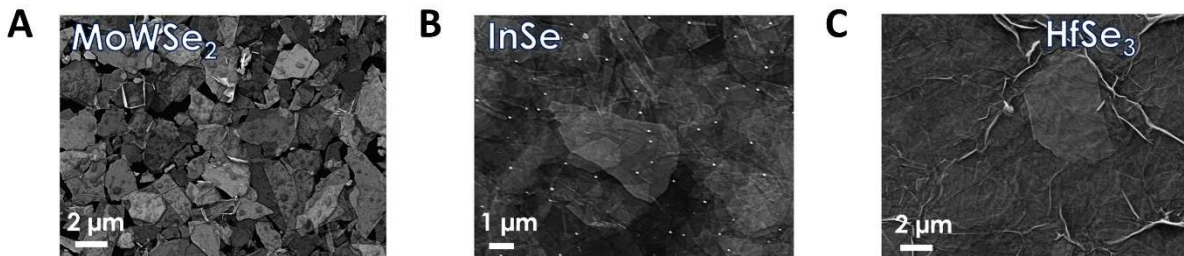


**Figure 8.** SEM images of novel materials, including  $\text{MoWSe}_2$ ,  $\text{InSe}$ , and  $\text{HfSe}_3$ .

Electrochemical exfoliation was also performed with tetraheptylammonium bromide (THAB) and acetonitrile (ACN) for crystals such as  $WS_2$ ,  $WSe_2$ ,  $Mo_{0.5}W_{0.5}Se_2$ , and Nb-doped  $MoSe_2$ . The production of atomic thin materials depends largely on the choice of the electrolyte solution. We explore the application of THAB/ACN electrolyte solution to yield monolayers for LEDs applications. There will be more materials to be tried in the future. The above listed materials are only our first attempts. The intercalation was conducted at 7 V and the intercalated crystals were subjected to ultra-sonication in a sonic bath for 30 min. The obtained dispersion was centrifuged to remove the unexfoliated particles. To examine the results, we performed photoluminescence (PL) measurement with a 532 nm laser. Those NSs exhibited PL will be further used for LEDs fabrications to examine their electroluminescence properties and basic characterisations such as UV-Vis absorption and morphological characterisations will also be performed. The PL measurement results are shown in Figure 9. PL peaks were found at 1.34 eV, 1.59 eV, 1.61 eV, and 1.82 eV for  $MoWSe_2$ ,  $WSe_2$ , Nb:WSe<sub>2</sub>, and  $WS_2$ , respectively.

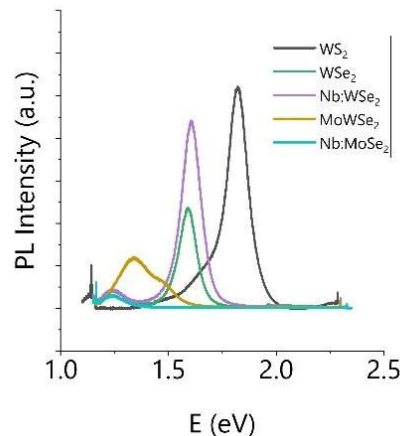


**Figure 9.** Photoluminescence measurement results of electrochemically exfoliated NSs.

At TUD,  $BiOCl$  NSs were produced by chemical exfoliation via alkali intercalation (Figure 10). Bulk  $BiOCl$  crystals were intercalated with electropositive reagents (Li, Na,  $NaH$ , and  $n$ -BuLi) in different solvents, targeting insertion between adjacent chlorine layers. This intercalation step expands/weakens the interlayer interactions, and a subsequent brief, low-power ultrasonication delaminates the material into high-aspect-ratio NSs, yielding stable dispersions.

Chemical exfoliation (CE) in a nutshell:

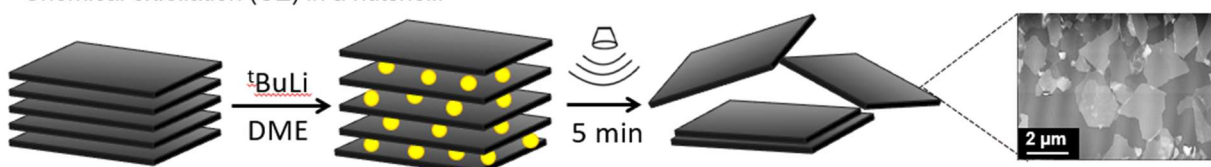


**Figure 10.** The schematic illustration of basic principles of chemical exfoliation.

Following this basic concept, TUD has been developing protocols for chemical exfoliation of BiOCl, a well-known photocatalysts and a potential dielectric materials suitable for application in 2D electronics. BiOCl crystalizes in tetragonal crystal system (space group 129) with Cl-Bi-O-Cl slabs being held together by weak van der Waals forces acting between adjacent Cl layers (Figure 11 a). Different combinations of intercalants and solvents are being tested, including in particular Li, Na and Li-organyls in different concentrations and solvents. The objective is to develop a method of exfoliation capable of producing colloidally stable NSs, while avoiding any decomposition. The preliminary results from experiments involving Na intercalation are very promising and indicate that the use Na source in the form of high reducing agent such as NaH in polar solvents such as H<sub>2</sub>O yields high aspect ratio NSs (Figure 11 b).

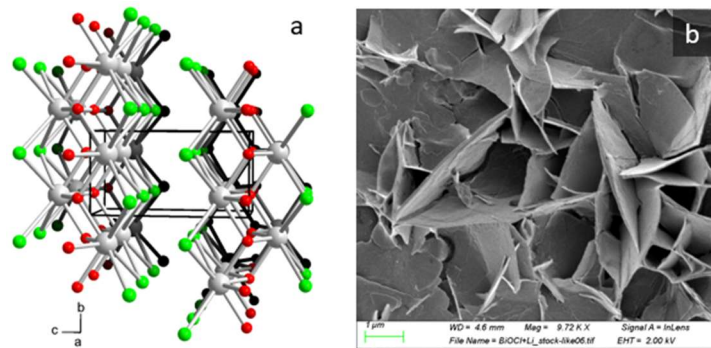


**Figure 11.** a) model of crystal structure of BiOCl. b) SEM image of BiOCl NSs exfoliated by ultrasonication following intercalation with NaH in water.

The advantage of chemical exfoliation using NaH is evident from Figure 12, which compares the NSs obtained by different methods including ultrasonication alone, and ultrasonication following intercalation by Li, Na or NaH in different solvents. The preliminary results clearly indicate that NaH holds greatest potential especially when chemical insertion of Na into BiOCl lattice is performed in the presence of water as solvent. In this case the bulk crystal exhibits high degree of delamination, which after ultrasonication yields high quality (panel g) NSs. On the contrary ultrasonication alone leads to very limited exfoliation of this material, yielding only thick platelets not suitable for printing of 2D electronics.

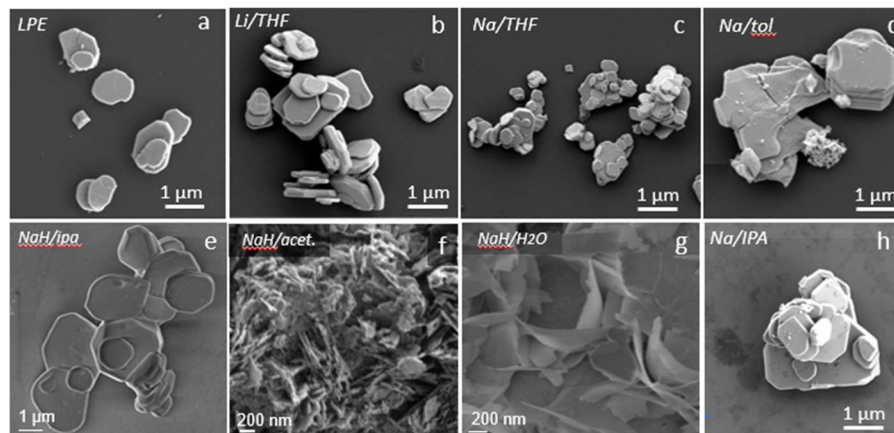


**Figure 12.** SEM images of BiOCl NSs obtained by different procedures involving either a) ultrasonication alone or ultrasonication following intercalation of bulk crystals by Li, Na or LiH in different solvents, as indicated on each panel.

UV-Vis spectra were recorded for all dispersions produced by CE, with LPE samples serving as reference. In Figure 13a, two fractions are compared: the sediment obtained after concentrating the dispersion by centrifugation, and the corresponding supernatant. Both spectra show features characteristic of BiOCl, with only minor differences. Figure 13b presents spectra of BiOCl treated with NaH in isopropanol, in which an additional absorption feature at  $\sim 270$  nm is observed. Nevertheless, the optical band gap remains unchanged within the resolution of the measurement. Figures 13c and 13d illustrate the impact of Na and NaH treatment in different solvents. Here, more pronounced spectral changes appear, suggesting partial decomposition of the material, possible phase transformations, or reduction processes induced during intercalation. These findings highlight the sensitivity of BiOCl to the choice of intercalant and solvent environment.

These results indicate that intercalation-assisted exfoliation of BiOCl represents a promising new pathway to access NS dispersions. However, the method is still highly sensitive to the choice of intercalant and solvent, and further systematic work will be required to achieve reproducibility and to better control the resulting NS quality and stability.

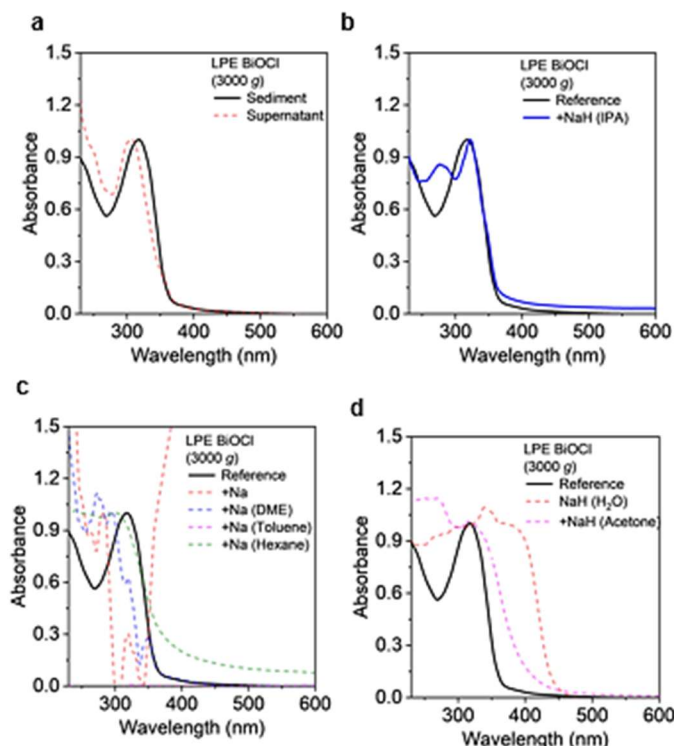


**Figure 13.** UV-Vis absorption spectra of chemically exfoliated BiOCl NSs. (a) Comparison of the sediment fraction (after centrifugation) and the corresponding supernatant. (b) BiOCl treated with NaH in IPA, showing an additional feature at  $\sim 270$  nm but no change in the optical band gap. (c, d) Spectra of BiOCl treated with Na and

*NaH in different solvents, exhibiting significant changes indicative for partial decomposition, phase transformation, or reduction of the starting material.*

### 3.3 Contribution to project (linked) Objectives

The progress made on production of 2D NSs described in this deliverable directly contributes to all the *materials objectives* of this project. At this stage more than 20 novel 2D materials have been developed and exfoliated to NS form through a variety of different methods. Among those we are focusing on sustainable and earth abundant materials for further optimisation. Using methodologies tailored for different materials, it was possible to achieve high aspect ratios of exfoliated NSs for most materials. Chemical modification methods are being developed to enable or improve the exfoliation of some bulk materials, as well as their stability and functionality for printing and application in different devices.

### 3.4 Contribution to major project exploitable result

The work described in this report adds to significant contribution already made across different WPs to several major project exploitable results. The materials being synthesized and exfoliated for the first time in WP1, some of which are reported here, are tailored for different applications and different components of all-printed devices. Many of these novel 2D materials are also being considered and tested for other applications, in particular energy storage/conversion-related applications. The feasibility of industrial scale production of selected materials has been demonstrated by us previously, indicating that 2D materials developed in this WP represent novel *products*, with specific properties and targeted applications. The exfoliation methodologies are continuously being developed and optimized for each of the novel materials selected, along with functionalization procedures that, for some materials, can be combined with the exfoliation step. Some of these methodologies can be directly translated to industrial scale production when needed; others will require modifications. Nevertheless, the methodologies described in this deliverable represent also the first reported *production processes* relating to the novel products/2D materials. Finally, the computational screening for novel 2D materials and synthesis of those in the bulk form within WP1 enables us to work with materials that have never or rarely been studied before even in the bulk form and whose properties and potential functionalities in low dimensional forms have not been experimentally assessed before. Nearly every aspect of this project, including the data reported in this deliverable, represents a groundbreaking *scientific discovery* that will be built upon by all project partners and serve as a base for future discoveries by others beyond the duration of this project.

## 4 Conclusion and Recommendation

This report updates on the progress made by WP1 partners on different methods of exfoliation used to produce nanosheets (NSs) from novel 2D materials theoretically identified and synthesized in bulk form within WP1. Three general methods of exfoliation have been used: Liquid phase exfoliation (LPE) based on ultrasonication alone, chemical exfoliation relying on chemical intercalation of bulk materials followed by delamination of intercalated material by ultrasonication, and finally electrochemical exfoliation. Additional method of LPE using a high shear mixer has also been explored in order to assess fast production of 2D NSs in larger quantities. The as-exfoliated materials were purified by centrifugation, often in several steps, to separate exfoliated from unexfoliated materials. Functionalization of some of the exfoliated materials has been achieved by having the surfactants present during the exfoliation stage.

Several transition metal oxyhalides, novel binary and ternary chalcogenides as well as some non-layered materials, have all been produced in 2D NS form by LPE. For some of the aforementioned materials even the use of high shear mixer allowed the production of appreciable quantities of NSs after a relatively short processing time, while for other materials the processing parameters used in preliminary experiments resulted in amorphization and degradation of the exfoliated material. Significant progress has been made with chemical (CE) and electrochemical exfoliation (EE) methods to obtain high aspect ratio of novel materials not achievable with sonication-assisted LPE. This was achieved by careful selection of solvents, intercalants or electrolytes and by tailoring carefully all other processing parameters. Further exploration and optimisation of those methods is ongoing. The produced materials are characterized by several techniques to ensure the quality of the exfoliated material and guide further optimization of the exfoliation methods. Some of the materials exfoliated in this project are sensitive to ambient degradation and, while some of this can be controlled and reduced by performing the critical production steps in inert atmosphere, in other cases we have taken advantage of the degradation processes that fortuitously enabled access to novel materials and their properties not accessible by exfoliation.

Future activities will focus on optimizing the production methods of selected materials, based on their potential application and to supply those to other partners for further functionalization, printing and device fabrication trials. In particular, CE and EE methods of producing high aspect NSs of different functionalities tailored for different components of all-printed device will continue to be developed and optimized, while sonication-assisted LPE can still serve as a simple method of assessing exfoliability of most materials, producing high quality NSs of other materials for which CE and EE methods are not suitable, and allow for testing different solvents and functionalization methodologies. For very selected few 2D materials, production upscaling to industrial level needs to be refined in terms of solvents used (the effectiveness of exfoliation versus safety limitations associated with their use in larger volumes in industrial setting), solvent exchange (in order to supply a 2D nanomaterial as dispersion ready and safe to use for specific applications) and solvent removal in order to obtain a pristine powder consisting of NSs of exfoliated 2D material.

## 5 References

- (1) Husremović, S.; Goodge, B. H.; Erodici, M. P.; Inzani, K.; Mier, A.; Ribet, S. M.; Bustillo, K. C.; Taniguchi, T.; Watanabe, K.; Ophus, C.; et al. Encoding multistate charge order and chirality in endotaxial heterostructures. *Nature Commun.* **2023**, *14* (1), 6031.
- (2) Synnatschke, K.; Shao, S.; Van Dinter, J.; Hofstetter, Y. J.; Kelly, D. J.; Grieger, S.; Haigh, S. J.; Vaynzof, Y.; Bensch, W.; Backes, C. Liquid exfoliation of Ni<sub>2</sub>P<sub>2</sub>S<sub>6</sub>: Structural characterization, size-dependent properties, and degradation. *Chem. Mater.* **2019**, *31* (21), 9127-9139.
- (3) John, B. B.; Andrew, H.; Ruiyuan, T.; Victor, V.-M.; Aideen, G.; Cian, G.; Madeleine, B.; Joshua, P.; Yanguang, L.; Jonathan, N. C. Liquid phase exfoliation of GeS nanosheets in ambient conditions for lithium ion battery applications. *2D Mater.* **2020**, *7* (3), 035015.
- (4) Hanlon, D.; Backes, C.; Doherty, E.; Cucinotta, C. S.; Berner, N. C.; Boland, C.; Lee, K.; Harvey, A.; Lynch, P.; Gholamvand, Z. Liquid exfoliation of solvent-stabilized few-layer black phosphorus for applications beyond electronics. *Nature Commun.* **2015**, *6* (1), 8563.
- (5) Vega-Mayoral, V.; Tian, R.; Kelly, A. G.; Griffin, A.; Harvey, A.; Borrelli, M.; Nisi, K.; Backes, C.; Coleman, J. N. Solvent exfoliation stabilizes TiS<sub>2</sub> nanosheets against oxidation, facilitating lithium storage applications. *Nanoscale* **2019**, *11* (13), 6206-6216.

## 6 Acknowledgement

The author(s) would like to thank the partners in the project for their valuable comments on previous drafts and for performing the review.

### Project partners:

#	Partner short name	Partner Full Name
1	TCD	TCD THE PROVOST, FELLOWS, FOUNDATION SCHOLARS & THE OTHER MEMBERS OF BOARD, OF THE COLLEGE OF THE HOLY & UNDIVIDED TRINITY OF QUEEN ELIZABETH NEAR DUBLIN
2	UNISTRA	UNIVERSITE DE STRASBOURG
3	UKa	UNIVERSITAET KASSEL
4	BED	BEDIMENSIONAL SPA
5	TUD	TECHNISCHE UNIVERSITAET DRESDEN
6	VSCHT	VYSOKA SKOLA CHEMICKO-TECHNOLOGICKA V PRAZE
7	UNR	UNIRESEARCH BV
8	UniBw M	UNIVERSITAET DER BUNDESWEHR MUENCHEN
9	EPFL	ECOLE POLYTECHNIQUE FEDERALE DE LAUSANNE

### Disclaimer/ Acknowledgment



Copyright ©, all rights reserved. This document or any part thereof may not be made public or disclosed, copied or otherwise reproduced or used in any form or by any means, without prior permission in writing from the 2D-PRINTABLE Consortium. Neither the 2D-PRINTABLE Consortium nor any of its members, their officers, employees or agents shall be liable or responsible, in negligence or otherwise, for any loss, damage or expense whatever sustained by any person as a result of the use, in any manner or form, of any knowledge, information or data contained in this document, or due to any inaccuracy, omission or error therein contained.

All Intellectual Property Rights, know-how and information provided by and/or arising from this document, such as designs, documentation, as well as preparatory material in that regard, is and shall remain the exclusive property of the 2D-PRINTABLE Consortium and any of its members or its licensors. Nothing contained in this document shall give, or shall be construed as giving, any right, title, ownership, interest, license or any other right in or to any IP, know-how and information.

This project has received funding from the European Union's Horizon Europe research and innovation programme under grant agreement No 101135196. Views and opinions expressed are however those of the author(s) only and do not necessarily reflect those of the European Union. Neither the European Union nor the granting authority can be held responsible for them.

## 7 Appendix A - Quality Assurance Review Form

The following questions should be answered by all reviewers (WP Leader, reviewer, Project Coordinator) as part of the Quality Assurance procedure. Questions answered with NO should be motivated. The deliverable author will update the draft based on the comments. When all reviewers have answered all questions with YES, only then can the Deliverable be submitted to the EC.

NOTE: This Quality Assurance form will be removed from Deliverables with dissemination level "Public" before publication.

Question	WP Leader	Reviewer	Project Coordinator	
	Francesco Bonaccorso (BeD)	Zdenek Sofer (VSCHT)	Xinliang Feng; Aliu Shaygan Nia (TUD)	Jonathan Coleman (TCD)
1. Do you accept this Deliverable as it is?	Yes	Yes	Yes	Yes
2. Is the Deliverable complete? - All required chapters? - Use of relevant templates?	Yes	Yes	Yes	Yes
3. Does the Deliverable correspond to the DoA? - All relevant actions preformed and reported?	Yes	Yes	Yes	Yes
4. Is the Deliverable in line with the 2D-PRINTABLE objectives? - WP objectives - Task Objectives	Yes	Yes	Yes	Yes
5. Is the technical quality sufficient? - Inputs and assumptions correct/clear? - Data, calculations, and motivations correct/clear? - Outputs and conclusions correct/clear?	Yes	Yes	Yes	Yes
6. Is created and potential IP identified and are protection measures in	Yes	Yes	Yes	Yes

place?				
7. Is the Risk Procedure followed and reported?	Yes	Yes	Yes	Yes
8. Is the reporting quality sufficient? - Clear language - Clear argumentation - Consistency - Structure	Yes	Yes	Yes	Yes